

Variational Quantum Algorithms for Gibbs State Preparation

Mirko Consiglio^[0000-0001-8730-0206]

Department of Physics, University of Malta, Msida MSD 2080, Malta
mirko.consiglio@um.edu.mt

Abstract. Preparing the Gibbs state of an interacting quantum many-body system on noisy intermediate-scale quantum (NISQ) devices is a crucial task for exploring the thermodynamic properties in the quantum regime. It encompasses understanding protocols such as thermalization and out-of-equilibrium thermodynamics, as well as sampling from faithfully prepared Gibbs states could pave the way to providing useful resources for quantum algorithms. Variational quantum algorithms (VQAs) show the most promise in efficiently preparing Gibbs states, however, there are many different approaches that could be applied to effectively determine and prepare Gibbs states on a NISQ computer. In this paper, we provide a concise overview of the algorithms capable of preparing Gibbs states, including joint Hamiltonian evolution of a system-environment coupling, quantum imaginary time evolution, and modern VQAs utilizing the Helmholtz free energy as a cost function, among others. Furthermore, we perform a benchmark of one of the latest variational Gibbs state preparation algorithms, developed by Consiglio et al. [16], by applying it to the spin 1/2 one-dimensional XY model.

Keywords: Quantum Computing · Quantum Algorithms · Quantum Thermodynamics

1 Introduction

Gibbs states (also known as thermal states) can be used for quantum simulation [12], quantum machine learning [6, 33], quantum optimization [58], and the study of open quantum systems [47]. Moreover, semi-definite programming [9], combinatorial optimization problems [58], and training quantum Boltzmann machines [33], can be tackled by sampling from well-prepared Gibbs states. Nevertheless, the preparation of an arbitrary quantum state on a quantum computer, is a QMA-hard problem [73]. Preparing Gibbs states, specifically at low temperatures, could be as hard as finding the ground-state of that Hamiltonian [2].

From a physical point of view, A Gibbs state is the quantum state that is at thermal equilibrium with the surrounding environment, in the canonical ensemble. Let's consider a Hamiltonian \mathcal{H} , describing n interacting qubits. The

Gibbs state at inverse temperature $\beta \equiv 1/k_B T$, where k_B Boltzmann constant and T is the temperature, is defined as

$$\rho(\beta, \mathcal{H}) = \frac{e^{-\beta\mathcal{H}}}{\mathcal{Z}(\beta, \mathcal{H})}, \quad (1)$$

where the partition function $\mathcal{Z}(\beta, \mathcal{H})$ is

$$\mathcal{Z}(\beta, \mathcal{H}) = \text{Tr}\{e^{-\beta\mathcal{H}}\} = \sum_{i=0}^{d-1} e^{-\beta E_i}. \quad (2)$$

Here the dimension $d = 2^n$, while $\{E_i\}$ are the eigenenergies of \mathcal{H} (with $\{|E_i\rangle\}$ denoting the corresponding eigenstates), i.e. $\mathcal{H}|E_i\rangle = E_i|E_i\rangle$.

While it may be a straightforward procedure to allow to allow a system to naturally thermalize with its environment, to obtain a Gibbs state, there is a great significance in being able to obtain a Gibbs of any arbitrary Hamiltonian. Since most physical systems are bound to specific types of Hamiltonian, a quantum computer can — at least in principle — simulate any arbitrary quantum system. Moreover, while a Gibbs distribution can be prepared on a classical computer, or even have a density matrix describing the Gibbs state stored on it, is not equivalent to having an actual Gibbs state on a quantum computer. Since we can continue to evolve, probe and simulate the Gibbs state to study quantum systems. As Richard Feynman aptly said [66], we require a quantum system to be able to effectively simulate, another, quantum system.

The objective of this study is twofold: firstly, to offer a comprehensive overview of Gibbs state preparation algorithms in Section 2, and to explore a noteworthy application of Gibbs states in quantum Boltzmann machines. Secondly, to present the recent variational Gibbs state preparation algorithm by Consiglio et al. [16] in Section 3. In Section 4, we apply the variational quantum algorithm (VQA) to prepare Gibbs states of the XY model, while also qualitatively investigating the scalability of the algorithm. Finally in Section. 5, we draw our conclusions.

2 Overview of Gibbs State Preparation Algorithms

The first computational technique one would usually resort to prepare a Gibbs state would be exact diagonalisation [30], however, since the full energy spectrum is needed, this method quickly becomes infeasible once the system size grows. A different approach is based on thermal pure quantum states [59, 60], which significantly reduces computational overhead when compared with exact diagonalisation. Nevertheless, since it requires preparing and evolving random quantum states, it is still limited in terms of system size. On the other hand, a quantum algorithm based on evaluating thermal pure shadows that operates using a quantum computer was proposed [18].

Initially, the first algorithms for preparing Gibbs states on a quantum computer were based on the idea of coupling the system to a register of ancillary

qubits, and letting the system and environment evolve under a joint Hamiltonian, simulating the physical process of thermalization [41, 54, 65]. Davies [19, 20] showed that, in the limits of small time-steps or weak system-bath interactions, the dynamics are described by a Lindblad master equation — the Davies generator — that thermalizes the system in the long-time limit. Nevertheless, implementing time-evolution on a noisy intermediate-scale quantum (NISQ) devices is currently impractical, since it requires long coherence times, and a significant number of ancilla qubits and/or precise qubit reset capabilities. One could resort to implementing the Davies generator directly on the quantum computer, however this would once again require applying quantum phase estimation [50] or other quantum subroutines related to the quantum Fourier transform [10]. Furthermore, Ref. [5] and Ref. [32] studied thermalization and Davies generators from the perspective of mathematical physics, showing rapid convergence to the Gibbs state and Gibbs distribution, respectively, under certain conditions. Ref. [8] devised a method for preparing the Gibbs state of a local Hamiltonian, assuming that the state has an exponential decay of correlations, and that it satisfies the approximate Markov condition uniformly on non-contractible regions. Ref. [78] also developed a quantum algorithm, based on a local quantum Markov process that can be used to sample from the Gibbs distribution.

Temme et al. [64] proposed the quantum Metropolis algorithm, that is capable of preparing Gibbs states through random walks, which is inspired from the Metropolis–Hastings algorithm [26, 42]. A quadratic speedup is achieved over the direct implementation of the Metropolis–Hastings algorithm by using Grover’s algorithm or related quantum algorithmic techniques [11, 47]. Using modern quantum algorithmic approaches, further polynomial speedups could be achieved, such as using dimension reduction to sample from Gibbs states [7], which requires the use of a precise quantum phase estimation subroutine, among others [14, 46, 74, 77]. A similar approach is the one in Ref. [51], which requires the use of a circuit very similar to that used in Shor’s algorithm [55], which can only be feasibly implemented on fault-tolerant quantum devices. Ref. [22] showed how to adapt “Coupling from the Past”-algorithms proposed by Ref. [49], to sample from the exact Gibbs distribution, rather than an approximation, using the quantum Metropolis algorithm. Nevertheless, compared with the local updates of the classical Metropolis algorithm, all of these algorithms require the implementation of large, global quantum circuits across the whole system, making them infeasible for NISQ devices. A recent review of current quantum Gibbs-sampling algorithms can be found in Ref. [10].

A promising approach for NISQ devices is that of VQAs, where a hybrid quantum–classical approach of minimizing an objective function, using a parametrized quantum circuit (PQC) as a variational ansatz, leads to the preparation of the Gibbs state. Some approaches utilize a physically-inspired objective function, the Helmholtz free energy, such in Refs. [13, 16, 21, 38, 53, 75]. Others employ an engineered cost function [48, 52], while others use quantum approximate optimization algorithm (QAOA)-based approaches [75, 79]. Alternative variational approaches consist of using: truncated Taylor series to

evaluate an approximation of the free energy [71]; adaptive derivative assembled problem-tailored (ADAPT)-VQA applied to a similar cost function to the free energy [72]; and a VQA based on McLachlan’s variational principle to initialize and evolve a thermofield double (TFD) state [34].

Alternative algorithms prepare thermal states through quantum imaginary time evolution (QITE), which typically require, either starting from a maximally mixed state [23, 40, 80], or a maximally entangled state [76], and carrying out imaginary time evolution of time τ , resulting in preparing the Gibbs state at inverse temperature β , that is directly proportional to τ . Refs. [24, 43, 61] utilize minimally entangled typical thermal states (METTS), in combination with QITE or measurement-based variational QITE to compute thermal averages and correlation functions of Hamiltonians. Ref. [63] developed a linear scaling QITE algorithm, called Fast QITE, that can also compute thermal averages. Ref. [70] also employed variational QITE, that is inspired from the measurement-based approach [43], however, it is adapted to be ansatz-based QITE. Ref. [56] utilizes random quantum circuits with intermediate measurements to impose QITE, while Ref. [57] proposed a fragmented QITE algorithm, for sampling from the Gibbs distribution.

Variational ansätze based on multi-scale entanglement renormalization [53] and product spectrum ansatz [38] have also been proposed in order to prepare Gibbs states. Other VQA approaches rely on variational quantum simulation [25, 69] and variational autoregressive networks [36]. The hybrid quantum–classical algorithms proposed in Ref. [37] differ from VQA, in that they compute microcanonical and canonical properties of many-body systems, using: filtering operators, similar to quantum phase estimation; and Monte Carlo simulations. Ref. [15] employs Green’s functions to sample from the Gibbs distribution. Finally, Ref. [27] proposed quantum-assisted simulation to prepare thermal states, which, contrary to VQAs, does not require a hybrid quantum–classical feedback loop.

One pertinent application of Gibbs states is quantum Boltzmann machines (QBMs) [3], which are a type of quantum machine learning model that are based on the principles of classical Boltzmann machines (CBMs) [1], but incorporate quantum effects such as entanglement and superposition. CBMs are variants of neural networks embedded in an undirected graph, where the weights and biases of the network represent the information encoded within it. Typically, the network consists of two groups of nodes: the visible nodes, that determine the input and output of the network; and the hidden nodes; which act as latent variables [80]. The purpose of training a Boltzmann machine is to learn the sets of weights and biases such that the resulting network is capable of approximating a target probability distribution, whereby the model learns by feeding in training data. The Boltzmann machine can then be used for both discriminative and generative learning [3].

A Boltzmann machine is represented by an undirected graph, where \mathbf{V} is the set of vertices (nodes) and \mathbf{E} is the set of edges. The states of the CBM are defined by $\mathbf{Z} = \{\mathbf{U}, \mathbf{H}\}$, where \mathbf{U} represents the state of the visible nodes, and

\mathbf{H} represents the state of the hidden nodes. This defines an energy function

$$E(\mathbf{Z}) = - \sum_{i \in \mathbf{V}} b_i z_i - \sum_{\{i,j\} \in \mathbf{E}} w_{ij} z_i z_j, \quad (3)$$

with $w_{ij} \in \mathbf{w}$, $b_i \in \mathbf{b}$, denoting the weights and biases (parameters) of the model, respectively. z_i is a binary unit, and to remain consistent with quantum mechanics, we define $z_i \in \{-1, 1\}$. Thus, the probability to observe a particular configuration \mathbf{U} of visible nodes is defined as

$$p_{\mathbf{U}} = \frac{1}{\mathcal{Z}(\beta, \mathbf{Z})} \sum_{\mathbf{H}} e^{-\beta E(\mathbf{Z})}, \quad (4)$$

where in this case,

$$\mathcal{Z}(\beta, \mathbf{Z}) = \sum_{\mathbf{Z}} e^{-\beta E(\mathbf{Z})}. \quad (5)$$

The Boltzmann distribution summed over the hidden variables in Eq. (4) is called the marginal distribution. The goal of a CBM is to determine the weights and biases of (3), such that $p_{\mathbf{U}}$ approximates well $p_{\mathbf{U}}^{\text{data}}$ defined by the training data. Typically, the cost function employed in the optimization procedure of a CBM is the Kullback-Leibler divergence, defined as

$$\mathcal{S}(p_{\mathbf{U}}^{\text{data}} \| p_{\mathbf{U}}) = \sum_{\mathbf{U}} p_{\mathbf{U}}^{\text{data}} \log p_{\mathbf{U}}^{\text{data}} - \sum_{\mathbf{U}} p_{\mathbf{U}}^{\text{data}} \log p_{\mathbf{U}}. \quad (6)$$

The main difference between a CBM and a QBM, is that the latter employs nodes that are defined by Pauli matrices rather than binary units, and therefore constructs a network defined by a parameterized Hamiltonian:

$$\mathcal{H}(\mathbf{b}, \mathbf{w}) = - \sum_{i \in \mathbf{V}} b_i \sigma_i^z - \sum_{\{i,j\} \in \mathbf{E}} w_{ij} \sigma_i^z \sigma_j^z. \quad (7)$$

In this case, the QBM is defined as the Gibbs state

$$\rho(\beta, \mathcal{H}) = \frac{e^{-\beta \mathcal{H}(\mathbf{b}, \mathbf{w})}}{\mathcal{Z}(\beta, \mathcal{H})}, \quad (8)$$

where

$$\mathcal{Z}(\beta, \mathcal{H}) = \text{Tr} \left\{ e^{-\beta \mathcal{H}(\mathbf{b}, \mathbf{w})} \right\}. \quad (9)$$

The cost function is thus the generalized Kullback-Leibler divergence for density matrices, which corresponds to the quantum relative entropy:

$$\mathcal{S}(\sigma \| \rho(\beta, \mathcal{H})) = \text{Tr} \{ \sigma \ln \sigma \} - \text{Tr} \{ \sigma \ln \rho(\beta, \mathcal{H}) \}, \quad (10)$$

where σ is the target density matrix representing the data embedded into a mixed state.

The goal of QBM training is to find a set of weights and biases of the Hamiltonian, such that the Gibbs state approximates the target density matrix. There are various methods of tackling the training of QBMs [18, 23, 29, 31, 80], and an analogous problem to QBM training is Hamiltonian learning [4].

3 Variational Gibbs State Preparation

Suppose one chooses a Hamiltonian \mathcal{H} and inverse temperature β . For a general state ρ , one can define a generalized Helmholtz free energy as

$$\mathcal{F}(\rho) = \text{Tr}\{\mathcal{H}\rho\} - \beta^{-1}\mathcal{S}(\rho), \quad (11)$$

where the von Neumann entropy $\mathcal{S}(\rho)$ can be expressed in terms of the eigenvalues, p_i , of ρ ,

$$\mathcal{S}(\rho) = - \sum_{i=0}^{d-1} p_i \ln p_i. \quad (12)$$

Since the Gibbs state is the unique state that minimizes the free energy of \mathcal{H} [39], a variational form can be put forward that takes Eq. (11) as an objective function, such that

$$\rho(\beta, \mathcal{H}) = \arg \min_{\rho} \mathcal{F}(\rho). \quad (13)$$

In this case, $p_i = \exp(-\beta E_i) / \mathcal{Z}(\beta, \mathcal{H})$ is the probability of getting the eigenstate $|E_i\rangle$ from the ensemble $\rho(\beta, \mathcal{H})$.

3.1 Computing the von Neumann Entropy

The difficulty in measuring the von Neumann entropy, defined by Eq. (12), of a quantum state on a NISQ device is typically the challenging part of variational Gibbs state preparation algorithms, since $\mathcal{S}(\rho)$ is not an observable. To exactly compute the von Neumann entropy on a quantum device, one would have to perform full state tomography on the Gibbs state, which has a time complexity of $\mathcal{O}(3^n)$ and a space complexity of $\mathcal{O}(4^n)$. As a consequence, different works have employed various techniques to compute an approximation for the von Neumann entropy, such as using: a Fourier series approximation to the von Neumann entropy [13]; a thermal multi-scale entanglement renormalization ansatz [53]; sums of Rényi entropies [21]; among others. On the other hand, Ref. [16] devised a method of computing the von Neumann exactly, via post-processing of measurement results acting on ancillary register.

When preparing an n -qubit state, the unitary gates used in quantum computers ensure that the final quantum state of the entire register, starting from the input state $|0\rangle^{\otimes n}$, remains pure. As a result, in order to prepare an n -qubit Gibbs state on the system register, an $m \leq n$ -qubit ancillary register is required. For example, in the case of the infinite-temperature Gibbs state, which is a fully mixed state, $m = n$ qubits are needed in the ancillary register to achieve maximal von Neumann entropy. To accurately evaluate the von Neumann entropy without any approximations, the complete Boltzmann distribution is prepared on the ancillary register, thus, $m = n$ is set regardless of the temperature.

3.2 Computing the Free Energy

Following the prescription of Ref. [16], we shall denote the ancillary register as A , while the preparation of the Gibbs state will be carried out on the system register S . The purpose of the VQA is to effectively create the Boltzmann distribution on A , which is then imposed on S , via intermediary CNOT gates, to generate a diagonal mixed state in the computational basis. In the ancillary register we can choose a unitary ansatz capable of preparing such a probability distribution. Thus, the ancillary qubits are responsible for classically mixing in the probabilities of the thermal state, while also being able to access these probabilities via measurements in the computational basis. On the other hand, the system register will host the preparation of the Gibbs state, as well as the measurement of the expectation value of our desired Hamiltonian during the optimization routine.

The specific design of the PQC allows classical post-processing of simple measurement results, carried out on ancillary qubits in the computational basis, to determine the von Neumann entropy. A diagrammatic representation of the structure of the PQC is shown in Fig. 1. Note that while the PQC of the algorithm has to have a particular structure — a unitary acting on the ancillae and a unitary acting on the system, connected by intermediary CNOT gates — it is not dependent on the choice of Hamiltonian \mathcal{H} , inverse temperature β , or the variational ansätze, U_A and U_S , employed within. This is in addition to enjoying a sub-exponential scaling in the number of shots needed to precisely compute the Boltzmann probabilities. A qualitative analysis of a power-law scaling is presented in Section 4.2.

3.3 Modular Structure of the PQC

The PQC, as shown in Fig. 1 for the VQA, is composed of a unitary gate U_A acting on the ancillary qubits, and a unitary gate U_S acting on the system qubits, with CNOT gates in between. Note that the circuit notation we are using here means that there are n qubits for both the system and the ancillae, as well as n CNOT gates that act in parallel, and are denoted as

$$\text{CNOT}_{AS} \equiv \bigotimes_{i=0}^{n-1} \text{CNOT}_{A_i S_i}. \quad (14)$$

The parametrized unitary U_A acting on the ancillae, followed by CNOT gates between the ancillary and system qubits, is responsible for preparing a probability distribution on the system. The parametrized unitary U_S is then applied on the system qubits to transform the computational basis states into the eigenstates of the Hamiltonian.

Throughout the paper we will describe unitary operations and density matrices in the computational basis: $\{|0\rangle, |1\rangle\}$, which is spanned by one qubit (and products of the basis states in the case of multiple qubits). A general unitary

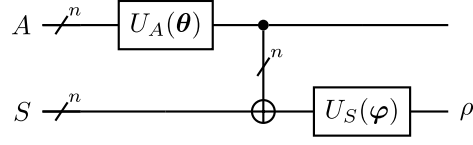


Fig. 1. PQC for Gibbs state preparation, with systems A and S each carrying n qubits. CNOT gates act between each qubit A_i and corresponding S_i .

gate of dimension $d = 2^n$ is given by

$$U_A = \begin{pmatrix} u_{0,0} & u_{0,1} & \cdots & u_{0,d-1} \\ u_{1,0} & u_{1,1} & \cdots & u_{1,d-1} \\ \vdots & \vdots & \ddots & \vdots \\ u_{d-1,0} & u_{d-1,1} & \cdots & u_{d-1,d-1} \end{pmatrix}. \quad (15)$$

Starting with the initial state of the $2n$ -qubit register, $|0\rangle_{AS}^{\otimes 2n}$, we apply the unitary gate U_A on the ancillae to get a quantum state $|\psi\rangle_A$, such that

$$(U_A \otimes I_S) |0\rangle_{AS}^{\otimes 2n} = |\psi\rangle_A \otimes |0\rangle_S^{\otimes n}, \quad (16)$$

where

$$|\psi\rangle_A = \sum_{i=0}^{d-1} u_{i,0} |i\rangle_A, \quad (17)$$

and I_S is the identity acting on the system. The next step is to prepare a classical probability mixture on the system qubits, which can be done by applying CNOT gates between each ancilla and system qubit. This results in a state

$$\text{CNOT}_{AS} \left(|\psi\rangle_A \otimes |0\rangle_S^{\otimes n} \right) = \sum_{i=0}^{d-1} u_{i,0} |i\rangle_A \otimes |i\rangle_S. \quad (18)$$

By then tracing out the ancillary qubits, we arrive at

$$\begin{aligned} & \text{Tr}_A \left\{ \left(\sum_{i=0}^{d-1} u_{i,0} |i\rangle_A \otimes |i\rangle_S \right) \left(\sum_{j=0}^{d-1} u_{j,0}^* \langle j|_A \otimes \langle j|_S \right) \right\} \\ &= \sum_{i,j=0}^{d-1} u_{i,0} u_{j,0}^* \langle i|j\rangle |i\rangle \langle j|_S \\ &= \sum_{i=0}^{d-1} |u_{i,0}|^2 |i\rangle \langle i|_S, \end{aligned} \quad (19)$$

ending up with a diagonal mixed state on the system, with probabilities given directly by the absolute square of the entries of the first column of U_A , that is,

$p_i = |u_{i,0}|^2$. If the system qubits were traced out instead, we would end up with the same diagonal mixed state,

$$\begin{aligned}
 & \text{Tr}_S \left\{ \left(\sum_{i=0}^{d-1} u_{i,0} |i\rangle_A \otimes |i\rangle_S \right) \left(\sum_{j=0}^{d-1} u_{j,0}^* \langle j|_A \otimes \langle j|_S \right) \right\} \\
 &= \sum_{i,j=0}^{d-1} u_{i,0} u_{j,0}^* \langle i|j\rangle |i\rangle\langle j|_A \\
 &= \sum_{i=0}^{d-1} |u_{i,0}|^2 |i\rangle\langle i|_A, \tag{20}
 \end{aligned}$$

This implies that by measuring in the computational basis of the ancillary qubits, we can determine the probabilities p_i , which can then be post-processed to determine the von Neumann entropy \mathcal{S} of the state ρ via Eq. (12) (since the entropy of A is the same as that of S). As a result, since U_A only serves to create a probability distribution from the entries of the first column, we can do away with a parametrized orthogonal (real unitary) operator, thus requiring less gates and parameters for the ancillary ansatz.

The unitary gate U_S then serves to transform the computational basis states of the system qubits to the eigenstates of the Gibbs state, such that

$$\begin{aligned}
 \rho &= U_S \left(\sum_{i=0}^{d-1} |u_{i,0}|^2 |i\rangle\langle i|_S \right) U_S^\dagger \\
 &= \sum_{i=0}^{d-1} p_i |\psi_i\rangle\langle\psi_i|, \tag{21}
 \end{aligned}$$

where the expectation value $\text{Tr}\{\mathcal{H}\rho\}$ of the Hamiltonian can be measured. Ideally, at the end of the optimization procedure, $p_i = \exp(-\beta E_i) / \mathcal{Z}(\beta, \mathcal{H})$ and $|\psi_i\rangle = |E_i\rangle$, so that we get

$$\rho(\beta, \mathcal{H}) = \sum_{i=0}^{d-1} \frac{e^{-\beta E_i}}{\mathcal{Z}(\beta, \mathcal{H})} |E_i\rangle\langle E_i|. \tag{22}$$

The VQA therefore avoids the entire difficulty of measuring the von Neumann entropy of a mixed state on a quantum computer, and instead transfers the task of post-processing measurement results to the classical computer, which is much more tractable.

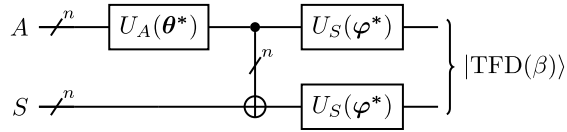


Fig. 2. Optimal PQC for TFD state preparation, with systems A and S each carrying n qubits. CNOT gates act between each qubit A_i and corresponding S_i .

3.4 Objective Function

Finally, we can define the objective function of our VQA to minimize the free energy (11), via our constructed PQC, to obtain the Gibbs state

$$\begin{aligned} \rho(\beta, \mathcal{H}) &= \arg \min_{\boldsymbol{\theta}, \boldsymbol{\varphi}} \mathcal{F}(\rho(\boldsymbol{\theta}, \boldsymbol{\varphi})) \\ &= \arg \min_{\boldsymbol{\theta}, \boldsymbol{\varphi}} (\text{Tr}\{\mathcal{H}\rho_S(\boldsymbol{\theta}, \boldsymbol{\varphi})\} - \beta^{-1}\mathcal{S}(\rho_A(\boldsymbol{\theta}))). \end{aligned} \quad (23)$$

It is noteworthy to mention that while the energy expectation depends on both sets of angles $\boldsymbol{\theta}$ (as U_A is responsible for parameterizing the Boltzmann distribution) and $\boldsymbol{\varphi}$ (as U_S is responsible for parameterizing the eigenstates of the Gibbs state), the calculation of the von Neumann entropy only depends on $\boldsymbol{\theta}$.

Furthermore, once we obtain the optimal parameters $\boldsymbol{\theta}^*$, $\boldsymbol{\varphi}^*$, preparing the Gibbs state $\rho(\beta, \mathcal{H})$ on the system qubits S , one can place the same unitary U_S with optimal parameters $\boldsymbol{\varphi}^*$ on the ancillary qubits to prepare the TFD state on the quantum computer, as shown in Fig. 2. A TFD state is defined as a pure state written in basis vectors $|i\rangle_A$ of system A , and $|\tilde{i}\rangle_B$ of system B :

$$|\text{TFD}(\beta, \mathcal{H})\rangle = \sum_{i=0}^{d-1} \sqrt{\frac{e^{-\beta E_i}}{\mathcal{Z}(\beta, \mathcal{H})}} |i\rangle_A \otimes |\tilde{i}\rangle_B. \quad (24)$$

Tracing out system A (B) yields the Gibbs state on system B (A). Notice that this is equivalent to Eq. (18) after applying U_S on both registers. Tracing out either the ancilla or system register yields the same Gibbs state on the other register.

4 Preparing Gibbs states of the XY model

In this Section we assess the performance of the VQA for Gibbs state preparation of an XY model. The XY model [35] is defined as

$$\mathcal{H} = - \sum_{i=1}^n \left(\frac{1+\gamma}{2} \sigma_i^x \sigma_{i+1}^x + \frac{1-\gamma}{2} \sigma_i^y \sigma_{i+1}^y \right) - h \sum_{i=1}^n \sigma_i^z. \quad (25)$$

Here we only report one relevant property for implementing a problem-inspired ansatz for U_S . The Hamiltonian in Eq. (25) commutes with the parity operator

$\mathcal{P} = \prod_{i=0}^{n-1} \sigma_i^z$. As a consequence, the eigenstates of \mathcal{H} have definite parity, and so will the eigenstates of ρ_β .

To assess the performance of the VQA, we utilize the Uhlmann-Josza fidelity as a figure of merit [67], defined as $F(\rho, \sigma) = (\text{Tr}\{\sqrt{\sqrt{\rho}\sigma\sqrt{\rho}}\})^2$. This fidelity measure quantifies the ‘‘closeness’’ between the prepared state and the target Gibbs state, making it a commonly-employed metric for distinguishability. However, alternative measures exist, each with its own interpretation. For instance, the trace distance [44] can be used, which guarantees that if its value between two states is bounded by ϵ , the expectation values computed on the effectively prepared state will differ from those of the true Gibbs state by at most an amount proportional to ϵ [28]. Another option is the relative entropy [44], which characterizes the distinguishability between the two states as the surprise that arises when an event occurs that is not possible with the true Gibbs state [68].

We use a simple, linearly entangled PQC for the unitary U_A , with parametrized $R_Y(\theta_i)$ gates, and CNOTs as the entangling gates. This ansatz is hardware efficient and is sufficient to produce real amplitudes for preparing the probability distribution. Note that we require the use of entangling gates [16], as otherwise we will not be able to prepare any arbitrary probability distribution, including the Boltzmann distribution of the XY model.

For the unitary U_S , We employ a brick-wall structure using parity-preserving gates — $R_{XY}(\varphi_i)$ followed by $R_{YX}(\varphi_j)$ gates. If we combine the two gates, which we denote as $R_P(\varphi_i, \varphi_j)$, we get

$$\begin{aligned} R_P(\varphi_i, \varphi_j) &= R_{YX}(\varphi_j) \cdot R_{XY}(\varphi_i) \\ &= \begin{pmatrix} \cos\left(\frac{\varphi_i + \varphi_j}{2}\right) & 0 & 0 & \sin\left(\frac{\varphi_i + \varphi_j}{2}\right) \\ 0 & \cos\left(\frac{\varphi_i - \varphi_j}{2}\right) - \sin\left(\frac{\varphi_i - \varphi_j}{2}\right) & 0 & 0 \\ 0 & \sin\left(\frac{\varphi_i - \varphi_j}{2}\right) & \cos\left(\frac{\varphi_i - \varphi_j}{2}\right) & 0 \\ -\sin\left(\frac{\varphi_i + \varphi_j}{2}\right) & 0 & 0 & \cos\left(\frac{\varphi_i + \varphi_j}{2}\right) \end{pmatrix}, \end{aligned} \tag{26}$$

which can be decomposed into two CNOT gates and six \sqrt{X} gates. One layer of the unitary acting on the system qubits consists of a brick-wall structure, composed of an even-odd sublayer of R_P gates, followed by an odd-even sublayer of R_P gates. Table 1 shows the scaling of the VQA assuming a closed ladder connectivity, for $n > 2$. An example of a PQC, split into a four-qubit ancilla register, and a four-qubit system register, is shown in Fig. 3.

4.1 Statevector Results

Fig. 4 shows the fidelity of the generated mixed state when compared with the exact Gibbs state of the XY model with $h = 0.5$, and γ ranging from 0.1 to 0.9 in steps of 0.1, across a range of temperatures for system sizes between two to seven qubits. The VQA was carried out using statevector simulations with the

Table 1. Scaling of the VQA assuming a closed ladder connectivity, for $n > 2$, where l_A and l_S are the number of ancilla ansatz and system ansatz layers, respectively, and P is 12 when n is even and 18 when n is odd.

# of parameters	$n(l_A + 1) + 2nl_S$	$\mathcal{O}(n(l_A + l_S))$
# of CNOT gates	$(n - 1)l_A + 2nl_S + n$	$\mathcal{O}(n(l_A + l_S))$
# of \sqrt{X} gates	$2n(l_A + 1) + 6nl_S$	$\mathcal{O}(n(l_A + l_S))$
Circuit depth	$(n + 1)l_A + Pl_S + 3$	$\mathcal{O}(nl_A + l_S)$

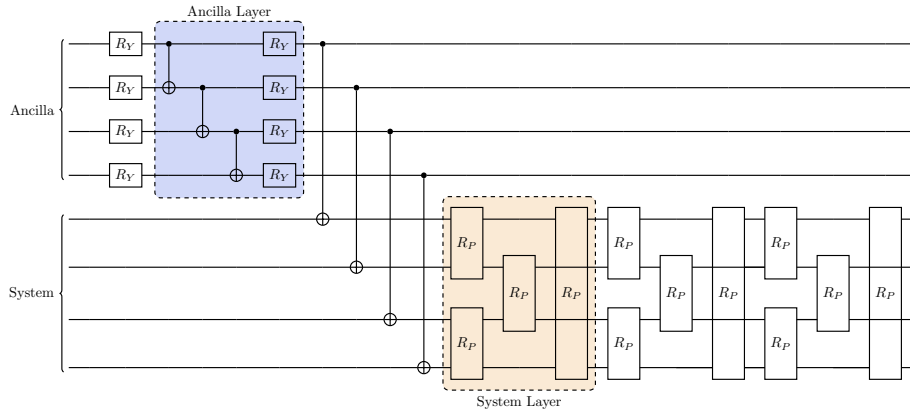


Fig. 3. Example of an eight-qubit PQC, consisting of one ancilla layer acting on a four-qubit register, and three $(n - 1)$ system layers acting on another four-qubit register. Each R_Y gate is parametrized with one parameter θ_i , while each R_P gate has two parameters φ_i and φ_j . The R_P gate is defined in Eq. (26). Note that the intermediary CNOT gates, as well as the R_P gates acting on qubits two and three, and on qubits one and four of the system, can be carried out in parallel, respectively.

Broyden–Fletcher–Goldfarb–Shanno (BFGS) optimizer [45]. We used one layer for the ancilla ansatz, and $n - 1$ layers for the system ansatz, with the scaling highlighted in Table 2. The number of layers was heuristically chosen to satisfy, at most, a polynomial scaling in quantum resources, while achieving a fidelity higher than 90% in statevector simulations. Furthermore, in order to alleviate the issue of getting stuck in local minima, the optimizer is embedded in a Monte Carlo framework, that is, taking multiple random initial positions and carrying out a local optimization from each position — which we call a ‘run’ — and finally taking the global minimum to be the minimum over all runs.

A total of 100 runs of BFGS per β were carried out (except for $n = 7$, where 10 were taken) to verify the reachability of the PQC, with Fig. 4 showcasing the maximal fidelity achieved for each β out of all runs. The results show that, indeed, our VQA, is able to reach a very high fidelity $F \gtrsim 90\%$ for up to seven-qubit Gibbs states of the XY model. In the case of the extremal points, that is $\beta \rightarrow 0$ and $\beta \rightarrow \infty$, the fidelity reaches unity, for all investigated system sizes. On the other hand, for intermediary temperatures $\beta \sim 1$, the fidelity decreases with

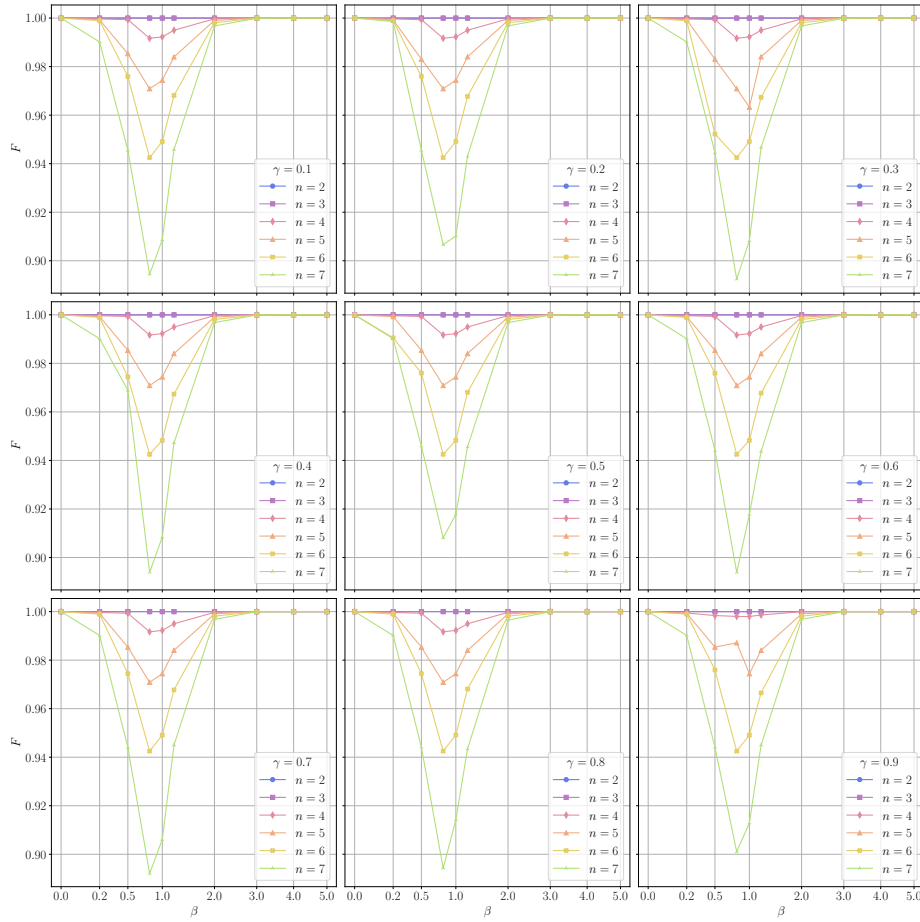


Fig. 4. Fidelity F , of the obtained state via statevector simulations (using BFGS) with the exact Gibbs state, vs inverse temperature β , for two to seven qubits of the XY model with γ between 0.1 and 0.9, and $h = 0.5$. A total of 100 runs are made for each point (except for $n = 7$, where 10 were taken), with the optimal state taken to be the one that maximizes the fidelity.

the number of qubits, which could be attributed to one layer of U_A not being expressible enough to prepare the Boltzmann distribution around intermediary temperatures (since the von Neumann entropy depends solely on $U_A(\theta)$ as in Eq. (23)).

4.2 Error Analysis

In this Section, we perform an analysis of the error scaling with the number of shots, in faithfully identifying the probability distribution,

Table 2. Scaling of the VQA assuming a closed ladder connectivity, for $n > 2$, with $l_A = 1$, and $l_S = n - 1$, and P is 12 when n is even and 18 when n is odd. The depth counts both CNOT and \sqrt{X} gates.

# of parameters	$2n^2$	$\mathcal{O}(n^2)$
# of CNOT gates	$2n^2 - 1$	$\mathcal{O}(n^2)$
# of \sqrt{X} gates	$2n(3n - 2)$	$\mathcal{O}(n^2)$
Circuit depth	$(P + 1)n - P + 4$	$\mathcal{O}(n)$

$\mathbf{p} = \{p_0, p_1, \dots, p_{d-1}\}$, where $d = 2^n$, prepared by U_A . The outcome of one shot of a quantum circuit can be described by a multinomial distribution, where p_i is the probability of observing a bit string i . The expected value of a multinomially distributed random bit string i is

$$\mu = \mathbb{E}[i] = np_i, \quad (27)$$

with the variance being

$$\sigma^2 = \text{Var}[i] = np_i(1 - p_i). \quad (28)$$

A quantity that can describe the precision of measuring the bit string i , p_i times, is the coefficient of variation, or relative standard deviation,

$$c_v = \frac{\sigma}{\mu} = \sqrt{\frac{1 - p_i}{N_s p_i}}. \quad (29)$$

Given that $p_i = \exp(-\beta E_i) / \mathcal{Z}(\beta, \mathcal{H})$ for the Boltzmann distribution, we get

$$c_v = \sqrt{\frac{1 - \frac{e^{-\beta E_i}}{\mathcal{Z}(\beta, \mathcal{H})}}{N_s \frac{e^{-\beta E_i}}{\mathcal{Z}(\beta, \mathcal{H})}}} = \sqrt{\frac{\mathcal{Z}(\beta, \mathcal{H}) - e^{-\beta E_i}}{N_s e^{-\beta E_i}}} = \sqrt{\frac{1}{N_s} \left(\frac{\mathcal{Z}(\beta, \mathcal{H})}{e^{-\beta E_i}} - 1 \right)}. \quad (30)$$

From Eq. (30), if $\beta \rightarrow 0$, then $\mathcal{Z}(\beta, \mathcal{H}) / \exp(-\beta E_i) \rightarrow d \forall i \in [d]$, which implies

$$c_v(\beta \rightarrow 0) = \sqrt{\frac{d - 1}{N_s}}, \quad (31)$$

hence, exhibiting an exponential scaling in the number of shots needed for preparing the flat distribution. On the other hand, if $\beta \rightarrow \infty$, then $\mathcal{Z}(\beta, \mathcal{H}) / \exp(-\beta E_0) \rightarrow 1$, while all other probabilities tend to zero, and the algorithm reduces to finding the ground-state of the Hamiltonian. As a result,

$$c_v(\beta \rightarrow \infty) = 0. \quad (32)$$

For intermediary temperatures, we carry out a qualitative analysis. Fig. 5 reports the exponent α_i , of a polynomial fit of the normalized coefficient of variation, defined as

$$c_v \sqrt{N_s} = C n^{\alpha_i}, \quad (33)$$

for n between 8 and 20, at different β , where the first 51 p_i of the XY model with $h = 0.5$, and γ between 0.1 and 0.9 are considered. We observe that as $\beta \rightarrow \infty$, the exponent α_0 approaches zero only for the ground-state occupation probability p_0 , in accordance with Eq. (32). Simultaneously, as the occupation probability p_i of an excited state decreases to negligible values, the corresponding exponent α_i becomes increasingly negative. However, for any finite temperature, we find that a polynomial fit, with $\alpha_i \lesssim 6$, provides a good approximation of the normalized coefficient of variation. This suggests that achieving a faithful reconstruction of the probability distribution, for the investigated system sizes of the XY model in NISQ algorithms, requires a sub-exponential scaling in the number of shots.

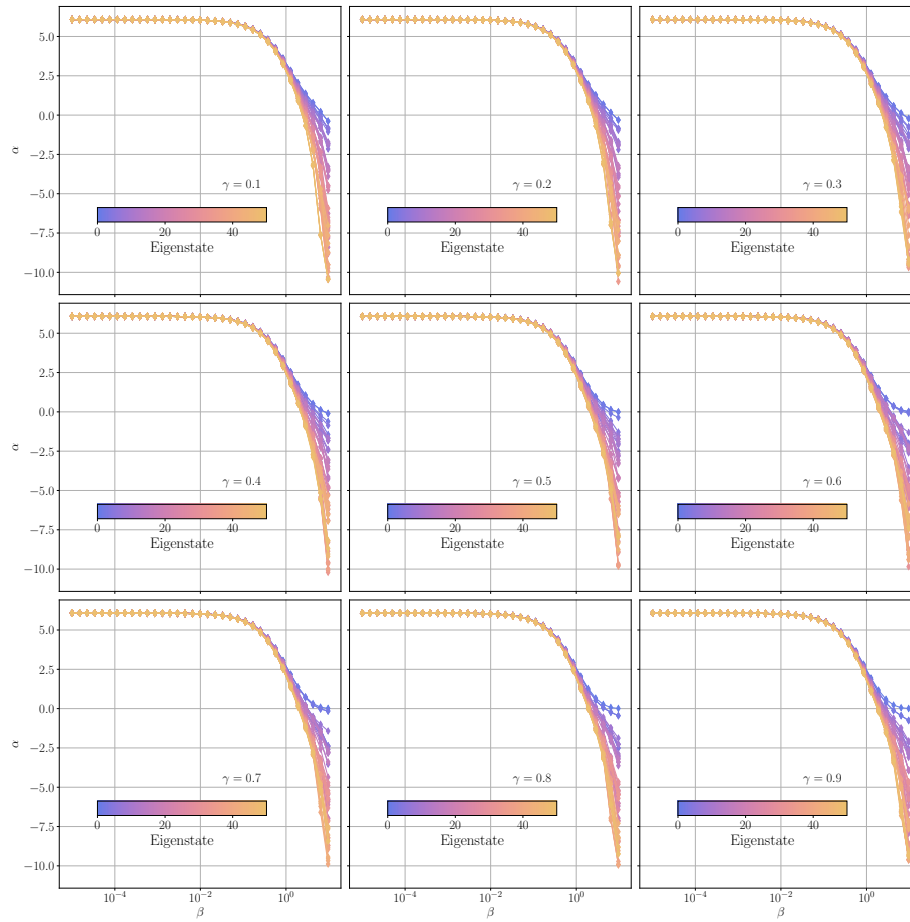


Fig. 5. The exponent α_i in Eq. (33) is plotted vs β for the first 51 p_i of the XY model with γ between 0.1 and 0.9, and $h = 0.5$, where each point is the polynomial fit for n between 8 and 20.

5 Conclusion

In this manuscript, we provided a concise overview of various Gibbs state preparation and Gibbs-sampling algorithms. However, our primary focus was on investigating VQAs for Gibbs state preparation. To accomplish this, we conducted a benchmark study using one of the latest variational Gibbs state preparation algorithms on the XY model, considering a wide range of temperatures and γ coefficients. Following the approach proposed by Consiglio et al. [16], we leveraged the unique property of the Gibbs state as the state that minimizes the Helmholtz free energy, which serves as an appropriate objective function for the VQA. Through extensive statevector simulations, we achieved fidelities of $F \gtrsim 90\%$ for system sizes up to seven qubits.

Furthermore, we performed a qualitative analysis of the scalability of the VQA for implementation on a NISQ device. We found that the number of gates, iterations, and shots scale at most polynomially with the number of qubits in the XY model. The algorithm’s scalability not only makes it suitable for near-term applications, but it holds significant potential for advancing quantum thermodynamic experiments on quantum computers, and ensuring the faithful preparation of Gibbs states for various computational tasks.

The Python code for running the statevector simulations, using Qulacs [62], can be found on GitHub [17].

Acknowledgments

MC would like to thank Jacopo Settino, Andrea Giordano, Carlo Mastroianni, Francesco Plastina, Salvatore Lorenzo, Sabrina Maniscalco, John Goold, and Tony J. G. Apollaro for fruitful and extensive discussions on Gibbs states, and the challenging task of variationally preparing them on NISQ computers. MC acknowledges funding by TESS (Tertiary Education Scholarships Scheme), and project QVAQT (Quantum Variational Algorithms for Quantum Technologies) REP-2022-003 financed by the Malta Council for Science & Technology, for and on behalf of the Foundation for Science and Technology, through the FUSION: R&I Research Excellence Programme.

References

1. Ackley, D.H., Hinton, G.E., Sejnowski, T.J.: A learning algorithm for boltzmann machines. *Cognitive Science* **9**(1), 147–169 (1985). [https://doi.org/10.1016/s0364-0213\(85\)80012-4](https://doi.org/10.1016/s0364-0213(85)80012-4)
2. Aharonov, D., Arad, I., Vidick, T.: Guest Column: The Quantum PCP Conjecture. *SIGACT News* **44**(2), 47–79 (Jun 2013). <https://doi.org/10.1145/2491533.2491549>
3. Amin, M.H., Andriyash, E., Rolfe, J., Kulchytskyy, B., Melko, R.: Quantum Boltzmann Machine. *Phys. Rev. X* **8**, 021050 (May 2018). <https://doi.org/10.1103/PhysRevX.8.021050>

4. Anshu, A., Arunachalam, S., Kuwahara, T., Soleimanifar, M.: Sample-efficient learning of interacting quantum systems. *Nature Physics* **17**(8), 931–935 (Aug 2021). <https://doi.org/10.1038/s41567-021-01232-0>
5. Bardet, I., Capel, A., Gao, L., Lucia, A., Pérez-García, D., Rouzé, C.: Rapid Thermalization of Spin Chain Commuting Hamiltonians. *Phys. Rev. Lett.* **130**, 060401 (Feb 2023). <https://doi.org/10.1103/PhysRevLett.130.060401>
6. Biamonte, J., Wittek, P., Pancotti, N., Rebentrost, P., Wiebe, N., Lloyd, S.: Quantum machine learning. *Nature* **549**(7671), 195–202 (Sep 2017). <https://doi.org/10.1038/nature23474>
7. Bilgin, E., Boixo, S.: Preparing thermal states of quantum systems by dimension reduction. *Phys. Rev. Lett.* **105**(17), 1–4 (2010). <https://doi.org/10.1103/PhysRevLett.105.170405>
8. Brandão, F.G.S.L., Kastoryano, M.J.: Finite Correlation Length Implies Efficient Preparation of Quantum Thermal States. *Communications in Mathematical Physics* **365**(1), 1–16 (Jan 2019). <https://doi.org/10.1007/s00220-018-3150-8>
9. Brandão, F.G.S.L., Svore, K.: Quantum Speed-ups for Semidefinite Programming (2016). <https://doi.org/10.48550/arxiv.1609.05537>
10. Chen, C.F., Kastoryano, M.J., ao, F.G.S.L.B., Gilyén, A.: Quantum Thermal State Preparation (2023). <https://doi.org/10.48550/arXiv.2303.18224>
11. Chiang, C.F., Wocjan, P.: Quantum Algorithm for Preparing Thermal Gibbs States - Detailed Analysis (2010). <https://doi.org/10.48550/arXiv.1001.1130>
12. Childs, A.M., Maslov, D., Nam, Y., Ross, N.J., Su, Y.: Toward the first quantum simulation with quantum speedup. *Proceedings of the National Academy of Sciences* **115**(38), 9456–9461 (2018). <https://doi.org/10.1073/pnas.1801723115>
13. Chowdhury, A.N., Low, G.H., Wiebe, N.: A Variational Quantum Algorithm for Preparing Quantum Gibbs States (2020). <https://doi.org/10.48550/arXiv.2002.00055>
14. Chowdhury, A.N., Somma, R.D.: Quantum algorithms for gibbs sampling and hitting-time estimation. *Quantum Inf. Comput.* **17**(1-2), 41–64 (2017). <https://doi.org/10.26421/qic17.1-2-3>
15. Cohn, J., Yang, F., Najafi, K., Jones, B., Freericks, J.K.: Minimal effective Gibbs ansatz: A simple protocol for extracting an accurate thermal representation for quantum simulation. *Phys. Rev. A* **102**, 022622 (Aug 2020). <https://doi.org/10.1103/PhysRevA.102.022622>
16. Consiglio, M., Settino, J., Giordano, A., Mastroianni, C., Plastina, F., Lorenzo, S., Maniscalco, S., Goold, J., Apollaro, T.J.G.: Variational Gibbs State Preparation on NISQ devices (2023). <https://doi.org/10.48550/arXiv.2303.11276>
17. Consiglio, Mirko: Variational Gibbs State Preparation. <https://github.com/mirkoconsiglio/VariationalGibbsStatePreparation> (2023)
18. Coopmans, L., Kikuchi, Y., Benedetti, M.: Predicting Gibbs-State Expectation Values with Pure Thermal Shadows. *PRX Quantum* **4**, 010305 (Jan 2023). <https://doi.org/10.1103/PRXQuantum.4.010305>
19. Davies, E.B.: Markovian master equations. *Communications in Mathematical Physics* **39**(2), 91–110 (Jun 1974). <https://doi.org/10.1007/bf01608389>
20. Davies, E.B.: Markovian master equations. II. *Mathematische Annalen* **219**(2), 147–158 (Jun 1976). <https://doi.org/10.1007/bf01351898>
21. Foldager, J., Pesah, A., Hansen, L.K.: Noise-assisted variational quantum thermalization. *Sci. Rep.* **12**(1), 3862 (Mar 2022). <https://doi.org/10.1038/s41598-022-07296-z>
22. França, D.S.: Perfect sampling for quantum Gibbs states. *Quantum Inf. Comput.* **18**(5-6), 361–388 (2018). <https://doi.org/10.26421/qic18.5-6-1>

23. Gacon, J., Zoufal, C., Carleo, G., Woerner, S.: Simultaneous Perturbation Stochastic Approximation of the Quantum Fisher Information. *Quantum* **5**, 567 (Oct 2021). <https://doi.org/10.22331/q-2021-10-20-567>
24. Getelina, J.C., Gomes, N., Iadecola, T., Orth, P.P., Yao, Y.X.: Adaptive variational quantum minimally entangled typical thermal states for finite temperature simulations (2023). <https://doi.org/10.48550/arXiv.2301.02592>
25. Guo, X.Y., Li, S.S., Xiao, X., Xiang, Z.C., Ge, Z.Y., Li, H.K., Song, P.T., Peng, Y., Wang, Z., Xu, K., Zhang, P., Wang, L., Zheng, D.N., Fan, H.: Variational quantum simulation of thermal statistical states on a superconducting quantum processor. *Chinese Physics B* **32**(1), 010307 (Jan 2023). <https://doi.org/10.1088/1674-1056/aca7f3>
26. Hastings, W.K.: Monte Carlo sampling methods using Markov chains and their applications. *Biometrika* **57**(1), 97–109 (1970). <https://doi.org/10.1093/biomet/57.1.97>
27. Haug, T., Bharti, K.: Generalized quantum assisted simulator. *Quantum Science and Technology* **7**(4), 045019 (Aug 2022). <https://doi.org/10.1088/2058-9565/ac83e7>
28. Holmes, Z., Muraleedharan, G., Somma, R.D., Subasi, Y., Şahinoğlu, B.: Quantum algorithms from fluctuation theorems: Thermal-state preparation. *Quantum* **6**, 825 (Oct 2022). <https://doi.org/10.22331/q-2022-10-06-825>
29. Huijgen, O., Coopmans, L., Najafi, P., Benedetti, M., Kappen, H.J.: Training Quantum Boltzmann Machines with the β -Variational Quantum Eigensolver (2023). <https://doi.org/10.48550/arXiv.2304.08631>
30. Jaklič, J., Prelovšek, P.: Lanczos method for the calculation of finite-temperature quantities in correlated systems. *Phys. Rev. B* **49**, 5065–5068 (Feb 1994). <https://doi.org/10.1103/PhysRevB.49.5065>
31. Kālis, M., Locāns, A., Šikovs, R., Naseri, H., Ambainis, A.: A hybrid quantum-classical approach for inference on restricted Boltzmann machines (2023). <https://doi.org/10.48550/arXiv.2304.12418>
32. Kastoryano, M.J., ao, F.G.S.L.B.: Quantum Gibbs Samplers: the commuting case (2016). <https://doi.org/10.48550/arXiv.1409.3435>
33. Kieferová, M., Wiebe, N.: Tomography and generative training with quantum Boltzmann machines. *Phys. Rev. A* **96**, 062327 (Dec 2017). <https://doi.org/10.1103/PhysRevA.96.062327>
34. Lee, C.K., Zhang, S.X., Hsieh, C.Y., Zhang, S., Shi, L.: Variational Quantum Simulations of Finite-Temperature Dynamical Properties via Thermofield Dynamics (2022). <https://doi.org/10.48550/arXiv.2206.05571>
35. Lieb, E., Schultz, T., Mattis, D.: Two soluble models of an antiferromagnetic chain. *Annals of Physics* **16**(3), 407–466 (1961). [https://doi.org/10.1016/0003-4916\(61\)90115-4](https://doi.org/10.1016/0003-4916(61)90115-4)
36. Liu, J.G., Mao, L., Zhang, P., Wang, L.: Solving quantum statistical mechanics with variational autoregressive networks and quantum circuits. *Machine Learning: Science and Technology* **2**(2), 025011 (Feb 2021). <https://doi.org/10.1088/2632-2153/aba19d>
37. Lu, S., Bañuls, M.C., Cirac, J.I.: Algorithms for Quantum Simulation at Finite Energies. *PRX Quantum* **2**, 020321 (May 2021). <https://doi.org/10.1103/PRXQuantum.2.020321>
38. Martyn, J., Swingle, B.: Product spectrum ansatz and the simplicity of thermal states. *Phys. Rev. A* **100**(3), 1–10 (2019). <https://doi.org/10.1103/PhysRevA.100.032107>

39. Matsui, T.: Purification and uniqueness of quantum Gibbs states. *Communications in Mathematical Physics* **162**(2), 321–332 (1994). <https://doi.org/10.1007/bf02102020>
40. McArdle, S., Jones, T., Endo, S., Li, Y., Benjamin, S.C., Yuan, X.: Variational ansatz-based quantum simulation of imaginary time evolution. *npj Quantum Information* **5**(1), 75 (Sep 2019). <https://doi.org/10.1038/s41534-019-0187-2>
41. Metcalf, M., Moussa, J.E., de Jong, W.A., Sarovar, M.: Engineered thermalization and cooling of quantum many-body systems. *Phys. Rev. Res.* **2**, 023214 (May 2020). <https://doi.org/10.1103/PhysRevResearch.2.023214>
42. Metropolis, N., Rosenbluth, A.W., Rosenbluth, M.N., Teller, A.H., Teller, E.: Equation of State Calculations by Fast Computing Machines. *The Journal of Chemical Physics* **21**(6), 1087–1092 (1953). <https://doi.org/10.1063/1.1699114>
43. Motta, M., Sun, C., Tan, A.T., O’Rourke, M.J., Ye, E., Minnich, A.J., Brandão, F.G., Chan, G.K.L.: Determining eigenstates and thermal states on a quantum computer using quantum imaginary time evolution. *Nat. Phys.* **16**(2), 205–210 (2020). <https://doi.org/10.1038/s41567-019-0704-4>
44. Nielsen, M.A., Chuang, I.L.: *Quantum Computation and Quantum Information: 10th Anniversary Edition*. Cambridge University Press (2010). <https://doi.org/10.1017/cbo9780511976667>
45. Nocedal, J., Wright, S.J.: *Numerical Optimization*. Springer, New York, NY, USA, 2e edn. (2006). <https://doi.org/10.1007/978-0-387-40065-5>
46. Ozols, M., Roetteler, M., Roland, J.: Quantum Rejection Sampling. In: *Proceedings of the 3rd Innovations in Theoretical Computer Science Conference*. p. 290–308. Ictcs ’12, Association for Computing Machinery, New York, NY, USA (2012). <https://doi.org/10.1145/2090236.2090261>
47. Poulin, D., Wocjan, P.: Sampling from the thermal quantum Gibbs state and evaluating partition functions with a quantum computer. *Phys. Rev. Lett.* **103**(22), 1–4 (2009). <https://doi.org/10.1103/PhysRevLett.103.220502>
48. Premaratne, S.P., Matsuura, A.Y.: Engineering a Cost Function for Real-world Implementation of a Variational Quantum Algorithm. In: *2020 IEEE International Conference on Quantum Computing and Engineering (QCE)*. pp. 278–285 (2020). <https://doi.org/10.1109/qce49297.2020.00042>
49. Propp, J.G., Wilson, D.B.: Exact sampling with coupled Markov chains and applications to statistical mechanics. *Random Structures & Algorithms* **9**(1-2), 223–252 (1996). [https://doi.org/10.1002/\(sici\)1098-2418\(199608/09\)9:1/2<223::aid-rsa14>3.0.co;2-o](https://doi.org/10.1002/(sici)1098-2418(199608/09)9:1/2<223::aid-rsa14>3.0.co;2-o)
50. Rall, P., Wang, C., Wocjan, P.: Thermal State Preparation via Rounding Promises (2022). <https://doi.org/10.48550/arXiv.2210.01670>
51. Riera, A., Gogolin, C., Eisert, J.: Thermalization in nature and on a quantum computer. *Phys. Rev. Lett.* **108**(8) (2012). <https://doi.org/10.1103/PhysRevLett.108.080402>
52. Sagastizabal, R., Premaratne, S.P., Klaver, B.A., Rol, M.A., Negîrneac, V., Moreira, M.S., Zou, X., Johri, S., Muthusubramanian, N., Beekman, M., Zachariadis, C., Ostroukh, V.P., Haider, N., Bruno, A., Matsuura, A.Y., DiCarlo, L.: Variational preparation of finite-temperature states on a quantum computer. *npj Quantum Inf.* **7**(1), 1–7 (2021). <https://doi.org/10.1038/s41534-021-00468-1>
53. Sewell, T.J., White, C.D., Swingle, B.: Thermal Multi-scale Entanglement Renormalization Ansatz for Variational Gibbs State Preparation (2022). <https://doi.org/10.48550/arXiv.2210.16419>

54. Shabani, A., Neven, H.: Artificial quantum thermal bath: Engineering temperature for a many-body quantum system. *Phys. Rev. A* **94**, 052301 (Nov 2016). <https://doi.org/10.1103/PhysRevA.94.052301>
55. Shor, P.: Algorithms for quantum computation: discrete logarithms and factoring. In: Proceedings 35th Annual Symposium on Foundations of Computer Science. pp. 124–134 (1994). <https://doi.org/10.1109/sfcs.1994.365700>
56. Shtanko, O., Movassagh, R.: Algorithms for Gibbs state preparation on noiseless and noisy random quantum circuits (2021). <https://doi.org/10.48550/arXiv.2112.14688>
57. Silva, T.L., Taddei, M.M., Carrazza, S., Aolita, L.: Fragmented imaginary-time evolution for early-stage quantum signal processors (2022). <https://doi.org/10.48550/arXiv.2110.13180>
58. Somma, R.D., Boixo, S., Barnum, H., Knill, E.: Quantum simulations of classical annealing processes. *Phys. Rev. Lett.* **101**(13), 1–4 (2008). <https://doi.org/10.1103/PhysRevLett.101.130504>
59. Sugiura, S., Shimizu, A.: Thermal Pure Quantum States at Finite Temperature. *Phys. Rev. Lett.* **108**, 240401 (Jun 2012). <https://doi.org/10.1103/PhysRevLett.108.240401>
60. Sugiura, S., Shimizu, A.: Canonical Thermal Pure Quantum State. *Phys. Rev. Lett.* **111**, 010401 (Jul 2013). <https://doi.org/10.1103/PhysRevLett.111.010401>
61. Sun, S.N., Motta, M., Tazhigulov, R.N., Tan, A.T., Chan, G.K.L., Minnich, A.J.: Quantum Computation of Finite-Temperature Static and Dynamical Properties of Spin Systems Using Quantum Imaginary Time Evolution. *PRX Quantum* **2**, 010317 (Feb 2021). <https://doi.org/10.1103/PRXQuantum.2.010317>
62. Suzuki, Y., Kawase, Y., Masumura, Y., Hiraga, Y., Nakadai, M., Chen, J., Nakanishi, K.M., Mitarai, K., Imai, R., Tamiya, S., Yamamoto, T., Yan, T., Kawakubo, T., Nakagawa, Y.O., Ibe, Y., Zhang, Y., Yamashita, H., Yoshimura, H., Hayashi, A., Fujii, K.: Qulacs: A fast and versatile quantum circuit simulator for research purpose. *Quantum* **5**, 559 (Oct 2021). <https://doi.org/10.22331/q-2021-10-06-559>
63. Tan, K.C.: Fast quantum imaginary time evolution (2020). <https://doi.org/10.48550/arXiv.2009.1223>
64. Temme, K., Osborne, T.J., Vollbrecht, K.G., Poulin, D., Verstraete, F.: Quantum Metropolis sampling. *Nature* **471**(7336), 87–90 (2011). <https://doi.org/10.1038/nature09770>
65. Terhal, B.M., DiVincenzo, D.P.: Problem of equilibration and the computation of correlation functions on a quantum computer. *Phys. Rev. A* **61**, 022301 (Jan 2000). <https://doi.org/10.1103/PhysRevA.61.022301>
66. Tralesinger, A.: Quantum simulation. *Nature Physics* **8**(4), 263–263 (Apr 2012). <https://doi.org/10.1038/nphys2258>
67. Uhlmann, A.: Transition Probability (Fidelity) and Its Relatives. *Foundations of Physics* **41**(3), 288–298 (2011). <https://doi.org/10.1007/s10701-009-9381-y>
68. Vedral, V.: The role of relative entropy in quantum information theory. *Rev. Mod. Phys.* **74**, 197–234 (Mar 2002). <https://doi.org/10.1103/RevModPhys.74.197>
69. Verdon, G., Marks, J., Nanda, S., Leichenauer, S., Hidary, J.: Quantum Hamiltonian-Based Models and the Variational Quantum Thermalizer Algorithm (2019). <https://doi.org/10.48550/arXiv.1910.02071>
70. Wang, X., Feng, X., Hartung, T., Jansen, K., Stornati, P.: Critical behavior of Ising model by preparing thermal state on quantum computer (2023). <https://doi.org/10.48550/arXiv.2302.14279>

71. Wang, Y., Li, G., Wang, X.: Variational Quantum Gibbs State Preparation with a Truncated Taylor Series. *Phys. Rev. Appl.* **16**(5), 1 (2021). <https://doi.org/10.1103/PhysRevApplied.16.054035>
72. Warren, A., Zhu, L., Mayhall, N.J., Barnes, E., Economou, S.E.: Adaptive variational algorithms for quantum Gibbs state preparation (2022). <https://doi.org/10.48550/arXiv.2203.12757>
73. Watrous, J.: Quantum Computational Complexity (2008). <https://doi.org/10.48550/arxiv.0804.3401>
74. Wocjan, P., Temme, K.: Szegedy Walk Unitaries for Quantum Maps (2021). <https://doi.org/10.48550/arXiv.2107.07365>
75. Wu, J., Hsieh, T.H.: Variational Thermal Quantum Simulation via Thermofield Double States. *Phys. Rev. Lett.* **123**(22), 1–7 (2019). <https://doi.org/10.1103/PhysRevLett.123.220502>
76. Yuan, X., Endo, S., Zhao, Q., Li, Y., Benjamin, S.C.: Theory of variational quantum simulation. *Quantum* **3**, 1–41 (2019). <https://doi.org/10.22331/q-2019-10-07-191>
77. Yung, M.H., Aspuru-Guzik, A.: A quantum-quantum Metropolis algorithm. *Proc. Natl. Acad. Sci. U. S. A.* **109**(3), 754–759 (2012). <https://doi.org/10.1073/pnas.1111758109>
78. Zhang, D., Bosse, J.L., Cubitt, T.: Dissipative Quantum Gibbs Sampling (2023). <https://doi.org/10.48550/arXiv.2304.04526>
79. Zhu, D., Johri, S., Linke, N.M., Landsman, K.A., Huerta Alderete, C., Nguyen, N.H., Matsuura, A.Y., Hsieh, T.H., Monroe, C.: Generation of thermofield double states and critical ground states with a quantum computer. *Proc. Natl. Acad. Sci. U. S. A.* **117**(41), 25402–25406 (2020). <https://doi.org/10.1073/pnas.2006337117>
80. Zoufal, C., Lucchi, A., Woerner, S.: Variational quantum Boltzmann machines. *Quantum Mach. Intell.* **3**(1), 1–15 (2021). <https://doi.org/10.1007/s42484-020-00033-7>